

# Using non-invasive non-destructive techniques to monitor cultural heritage objects

D Thickett, C S Cheung, H Liang, J Twydle, R Gr Maev and D Gavrilov

*Cultural heritage plays a significant role in our identities and well-being. The aim of conservation is to manage change to cultural heritage objects. Non-destructive techniques offer an opportunity to quantify deterioration objectively and at an earlier stage than observation. There are limitations for using the techniques on precious artefacts. This paper examines some of the issues and opportunities through case studies with phased pulse thermography, acoustic emission, Fourier transform infrared spectroscopy and optical coherence tomography, applied to a series of mediaeval Limoges enamel plaques from the Werner Collection, displayed at Rangers House, London.*

## Introduction

Cultural heritage plays a significant role in our identities and well-being. The aim of conservation is to manage change to cultural heritage objects<sup>[1]</sup>. This deterioration has traditionally been monitored through visual surveys (often with magnification and UV/IR) by highly-trained conservators. However, deterioration is not always readily observable and there are known issues with inter-observer bias. Non-destructive techniques offer an opportunity to quantify deterioration objectively and at an earlier stage than observation. There are limitations for using the techniques on precious artefacts. The high insurance costs and risks of moving valuable cultural heritage objects mean portable systems are preferable. This paper examines some of the issues and opportunities through case studies of a series of mediaeval Limoges enamel plaques from the Werner Collection, displayed at Rangers House, London.

For enamels with multiple glass layers over copper plate, the main deterioration mechanisms are physical and chemical. The differences between the thermal expansion coefficient of the copper and glass mean temperature changes cause stress. This can lead to debonding between the glass and metal. In extreme circumstances, this can cause pieces of glass to fly off the object. Whilst such instances have been reported, there has been no systematic research in this area to determine safe or damaging temperature fluctuations. There is little scientific data on the thermal expansion coefficients of the glass compositions used in ancient enamels and their often complex structure makes mechanical modelling to determine damage thresholds difficult, even with sufficient data. Certain glass compositions used in mediaeval enamels are inherently chemically unstable. The glass reacts with airborne moisture and sodium and potassium ions are replaced with water-derived ions. This generates a layer of what is essentially a silica gel on the glass surface. The layer, when thick enough, is visually disfiguring. The layer is also hygroscopic and can crack if the relative humidity (RH) drops too low. This limits the main preventative conservation strategy to conserve the glass, keeping it at a low RH value<sup>[2]</sup>.

## Principal component thermography

The grisaille enamel plaque by Penicaud, EE 133 A, from the 16th century, cracked while on display in 2006 and several small pieces of enamel were collected from the showcase. This was associated with a 5°C rise in temperature in the showcase. Monitoring of the

piece is complicated as the high-gloss black enamel is very difficult to photograph and, even with photography, it is difficult to monitor changes in the cracks present.

The object was subjected to xenon flashes and the IR image captured with a coupled FLIR SC4000 camera. As the object is prone to thermal damage, the temperature gain on a black glass surface was determined using a Pt100 probe and SR-002 datalogger (1 ms interval). With the experimental set-up used, this was below 1.7°C. The enamels have been exposed to such a change over 100 times per year for the past decade, so the risk to the enamel was considered acceptable. Principal component thermography utilises statistical processing of raw sequences of collected thermal images by representing them in a multidimensional space formed by a number of dimensions of each image. The procedure utilised in this process allows a few images to be found that represent the independent statistical modes among all the collected images. In simple terms, these newly found images (called principal components (PCs)) represent a set of patterns that form the thermal images sorted with respect to their influence. For example, the first PC usually corresponds to the non-uniformity of heating, because it is present in all the images collected in the thermographic experiment. The second one (PC2) already shows deviations from the pattern formed by the non-uniformity of heating. This makes it very promising for defect detection. In practice, principal components with orders of two to about six show the defects and internal structure, while the higher components (PC7 and higher) mostly show thermal and instrumental noise images.

The principal component thermography produced clear images of the cracks present at different depths in the enamel plaque. Repeating

### Submitted 18.12.16 / Accepted 06.02.17

*Based on a paper presented at the 'Analysing Art: New Technologies and Applications' workshop, held 19-20 May 2016, London, UK*

*David Thickett is with English Heritage, Rangers House, Chesterfield Walk, London SE10 8QX, UK.*

*Chi Shing Cheung and Haida Liang are with the School of Science & Technology, Nottingham Trent University, Nottingham NG11 8NS, UK.*

*John Twydle is with The True Image Solution, Enterprise Way, Edenbridge, Kent TN8 6HF, UK.*

*Roman Gr Maev and Dmitry Gavrilov are with the Department of Physics, University of Windsor, Windsor, N9B 3P4, Canada.*



Figure 1. Limoges enamel plaques painted in grisaille after Caraglio by Penicaud, EE 133 A

©The Wernher Foundation. Source: Historic England Photo Library

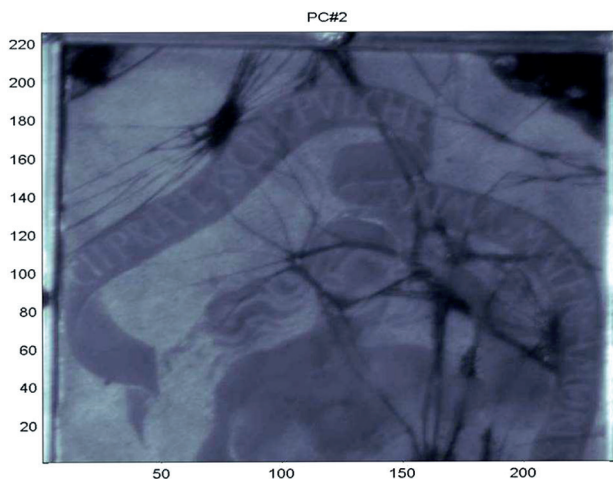


Figure 2. Principal component No 2 extracted from thermography

the process will allow any extension or new cracks to be identified. Controlling the geometry and settings for the equipment, combined with observing decoration from the object in the thermograms, allows for an accurate comparison of the images obtained at different times. However, if change is detected within a certain period, there will be uncertainty as to which of the temperature fluctuations actually contributed towards the observed damage. Direct tracing methods that record damage at a time interval similar to that used to monitor the environment are available.

## Acoustic emission

Acoustic emission has been used to monitor the debonding at the glass/metal interface described previously. A Physical Acoustics Pocket AE2 with two R15α sensors (1 kHz to 1 MHz, ±1.5 dB) was used. Measurements with contact gel were made on simulated weathered enamels, kindly provided by Veerle Van der Linden and Eva Annys from the Royal Academy of Fine Arts, University of Antwerp, Belgium. As contact gel could not be used on art objects, experiments were undertaken with different materials clamped between the sensor and the replica enamel and the amplitude of pencil break tests<sup>[3]</sup> was used to assess the most suitable material. A 75 μm film of Melinex was found to transmit the highest amplitude. This material has a long history of use in conservation and has been extensively tested to ensure it has no adverse effects on artefacts.

Several enamels were monitored for periods of three to five days. One sensor was clamped to the back of the enamel and one to the front with Melinex between the sensor and enamel surface. The mounted sensors were held in laboratory clamps and the heavy baseboard positioned so that the sensor was pushed against the enamel. Pencil break tests were used to assess the transit time for acoustic emission signals through the depth of the enamel. Any signals detected on the two sensors at intervals greater than the transit time were taken to be noise. As the front sensor obscured the enamel surface, monitoring for a longer period was not possible. The large number of noise events (originating outside the enamel) unfortunately precluded the possibility of just having a sensor on the back of the enamel, which would have been more visually acceptable. This limitation depends on the size of the object and acoustic emission has been successfully used for large sculptures and wooden furniture<sup>[4,5]</sup>. Figure 3 shows one set of results from the acoustic emission monitoring. Only events originating within the enamel are shown. The events only occurred when the air temperature increased and began after an increase of approximately 2°C. Further investigation indicated that the tungsten showcase lighting was driving much of the temperature gain. This was replaced with LED lights, which reduced the temperature gain throughout most of the year and no acoustic emission was observed. Summer still induced some acoustic emission and a chiller unit was installed in the room to stabilise the temperature. No further acoustic emission events were observed after this was installed.

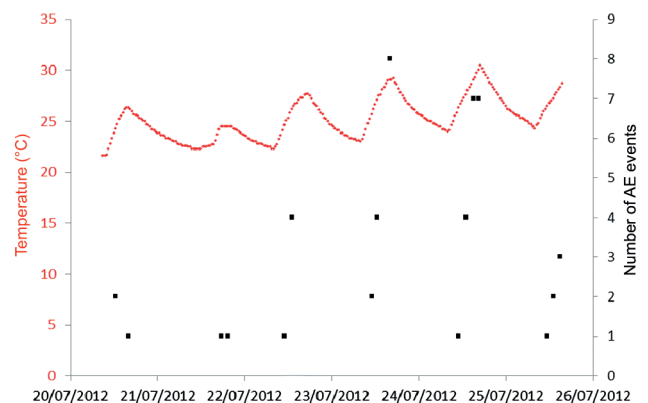


Figure 3. AE from enamel

The main advantage of acoustic emission monitoring is that its timeframe is such that it can be directly related to observed changes in the environment.



## Fourier transform infrared (FTIR) microscopy

The increasing depth of the gel layer on the surface of the glass is the primary consequence of chemical weathering of enamels. Thicker gel layers alter the appearance of the glass (the primary artistic intent) and thicker layers respond to fluctuating RH and can crack. The cracking exposes more undegraded glass to the atmosphere and accelerates the reaction. Characterising this gel layer is critical to monitoring such objects. A number of techniques have the potential to achieve this. Some gel layers, especially for highly coloured enamels, can be discerned by eye. In these cases, measuring microscopes or 3D confocal microscopy can determine the layer depth. However, in many instances the gel cannot be distinguished from the glass. Infrared spectroscopy, infrared reflection-absorption (IRAS) microscopy and reflectance spectroscopy have all been used to characterise the gel layer thickness. As the gel layer forms, Si-O-Si bonds break to Si-OH and Si-O-Na bonds, which can be observed at characteristic wavenumbers ( $990\text{ cm}^{-1}$  and  $950\text{ cm}^{-1}$ ) in infrared spectra<sup>[6]</sup>. Confocal micro-Raman spectroscopy has also been used to determine the depth of gel layers on glass<sup>[7]</sup>. In this work, a Nicolet Inspect IR microscope was used running off a Nicolet Avatar 360 bench. This fixed-focus instrument collected a spectrum from a  $100\text{ }\mu\text{m}$ -diameter circle at  $1\text{ cm}^{-1}$  resolution. The microscope allows viewing of a  $500\text{ }\mu\text{m}$  square and Melinex masks with  $200\text{ }\mu\text{m}$  holes carefully pierced through the Melinex allowed accurate repositioning of the analysis. Four sets of analysis were undertaken over a 12-year period. The stability of the instrument over this period was checked with glass standards and the information depth determined to be between  $1.78\text{ mm}$  and  $2.04\text{ mm}$ <sup>[6]</sup>. The information depth is important. If it is less than the depth of the glass, then only information on the surface gel layer is acquired. If it is greater than the depth of the glass, both the outer (glass/air surface) and inner (glass/metal surface) gels contribute to the signal. Four enamels were monitored, including that shown in Figure 4.

15 points were measured on each different coloured area of enamel, away from the edges of the area where other enamels may



Figure 4. *The Betrayal of Christ by the Monvaerni Master, circa 1480, EE 328*

©The Wernher Foundation. Source: Historic England Photo Library

be underneath. Any spectra with anomalous peak shapes were discarded. Each measurement had over 11 useable spectra. The peak splitting distance between the Si-OH peak and Si-O-Na peak was used as a measure of the deterioration. Several colours showed no observable deterioration, but the blues and purples both showed a statistically significant increase in the peak splitting value.

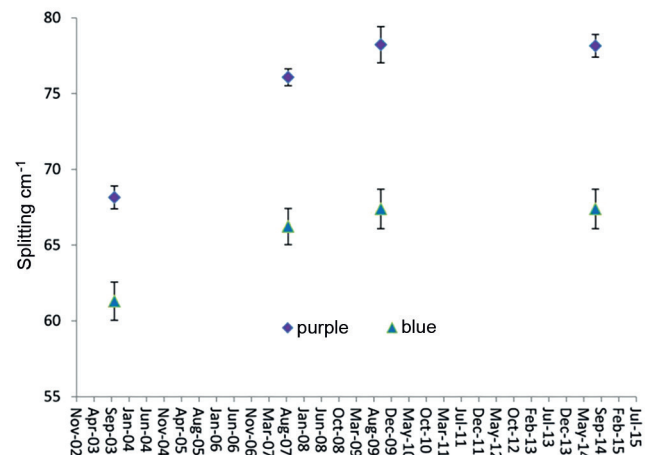


Figure 5. Splitting values of Si-O peak for purple and blue enamel areas from FTIR microscopy; error bars are three standard deviations

The two enamel colours probably behave differently due to their different glass compositions; this was investigated later.

A variety of interventions improved the environment. Between 2003 and 2007, the showcase spent over 13% of the time above 42% RH (the target value). The type of silica gel was changed in September 2007, but the case still spent 3% of the time above 42% RH. The increase in splitting for the purple enamel was still statistically significant after this intervention. In late 2009, a mechanical control system was added that maintained the RH below 42%.

Closer examination of the FTIR results showed that within a single colour area, certain measurement points were consistently above or below the mean value, perhaps indicating less variation than the errors imply. The values for each point are included in Figure 6.

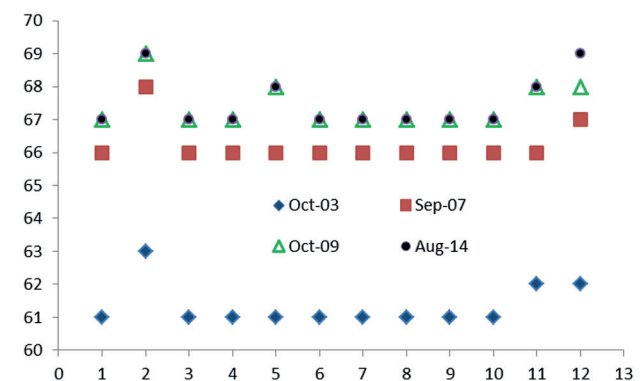


Figure 6. Point-by-point FTIR of blue enamel area

These results indicate a systematic variation in the glass composition. Air-path X-ray fluorescence (XRF) was undertaken at the approximate locations. The XRF analyser was a modified Link Analytical 290 spectrometer incorporating a molybdenum target X-ray tube operated at 25 kV. The positioning laser was placed

on the hole in the Melinex mask and the mask was then removed and analysis undertaken. The analytical area of the XRF was an ellipse with a minor axis of 1 mm and a major axis of 2 mm. This is obviously much larger than the FTIR microscope's area. The system was calibrated with standard glass samples representing historic glass compositions<sup>[9]</sup>. The results are shown in Table 1.

Table 1. Blue enamel semi-quantitative XRF

	Si	K	Ca	Fe	Mo	Cu	Ni	Zn	Pb	Total
1	69.23	9.3	4.98	0.38	7.2	0.14	0.02	0.06	1.17	92.48
2	68.46	9.17	5.54	0.39	7.40	0.08	0.02	0.08	2.45	93.58
3	69.62	9.21	4.99	0.39	7.33	0.07	0.03	0.08	1.33	93.01
4	69.28	9.15	5.07	0.44	7.32	0.07	0.02	0.07	1.24	92.66
5	69.50	9.14	5.02	0.46	7.25	0.05	0.01	0.07	1.26	92.75
6	69.48	9.16	4.92	0.38	7.39	0.05	0.02	0.08	1.23	92.69
7	69.43	9.26	5.00	0.44	7.32	0.06	0.03	0.07	1.23	92.80
8	69.53	9.13	4.96	0.44	7.25	0.07	0.02	0.07	1.20	92.65
9	69.49	9.21	4.91	0.45	7.29	0.12	0.04	0.06	1.30	92.83
10	69.24	9.20	4.91	0.40	7.26	0.11	0.02	0.08	1.28	92.47
11	69.30	9.26	3.45	0.44	7.22	0.05	0.02	0.07	1.96	91.75

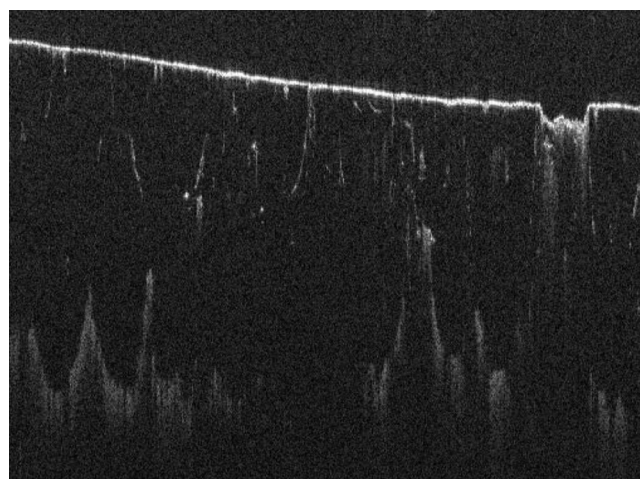
The results are semi-quantitative as the important element, silicon, cannot be fully quantified due to absorption of its X-rays in the air path and sodium (which is known to be present) cannot be detected at all. The presence of an undetected element is indicated by the total percentages summing to significantly less than 100. A significant variation in calcium and lead was observed. These elements are important in glass stability as they act as network stabilisers. Counterintuitively, the most degraded areas of the blue glass have the highest concentrations of network stabilisers. Unfortunately, the missing elemental information from air-path XRF precludes a full analysis. The mismatch in sample areas between the two techniques also makes comparison difficult. XRF analyses of the purple enamel indicated lower calcium and lead concentrations, consistent with the greater degradation observed.

### Optical coherence tomography

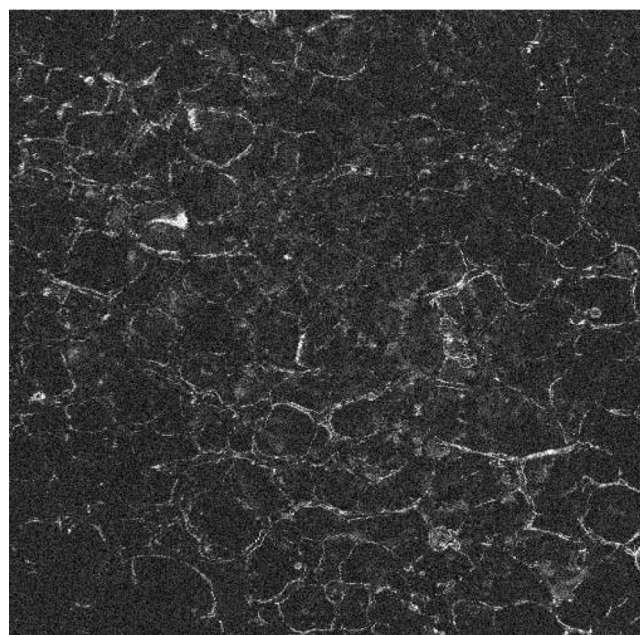
Optical coherence tomography (OCT) is an imaging white light interferometer capable of non-contact surface and subsurface 3D imaging of microstructures. A recent AHRC/EPSRC research project developed OCT instrumentation optimised towards cultural heritage applications<sup>[10,11]</sup>. This included an ultra-high-resolution OCT (UHR OCT) with an axial resolution of 1.2 microns (in glass) for the highest resolution to distinguish thin layers<sup>[10]</sup> and a long-wavelength OCT with a central wavelength of 1960 nm for deeper penetration into highly scattering material<sup>[11]</sup>. In this work, UHR OCT was used to examine the gel layers and internal structures of the enamel. The UHR OCT operating at a central wavelength of 810 nm has a depth resolution of 1.2 microns in glass, a transverse resolution of 7 microns and is capable of collecting a 3D image cube of a 5 mm by 5 mm area at a transverse sampling resolution of 10 microns in 10 s<sup>[10]</sup>.

A virtual cross-section image and a virtual cut parallel to the surface of the bottom right blue drapery in the enamel shown in Figure 4 are shown in Figures 7(a) and 7(b), respectively.

The top surface clearly shows a surface crack and an interrupted gel layer just below the surface. The variable gel layer thickness is consistent with the XRF and FTIR results.



(a)



(b)

Figure 7. (a) OCT virtual cross-section image (5 mm wide and 0.57 mm deep) of the bottom right blue drapery region of the enamel shown in Figure 4; (b) the corresponding virtual thin slice (5 mm by 5 mm) parallel to and just below the enamel surface showing the interrupted gel layer network

### Conclusions

Non-destructive techniques have significantly improved the monitoring of Limoges enamel plaques. They have provided evidence to alter the display environment, replacing lighting and adding chilling to limit temperature fluctuations. The techniques have had to be checked, with the thermal gain being monitored during phased pulse thermography, altered and contact gel being replaced with Melinex for acoustic emission, and developed, with the use of higher-resolution OCT to allow optimum application on cultural heritage objects. Numerous other beneficial applications can be foreseen and this is a rapidly expanding field.

### References

1. English Heritage Conservation Principles, 'Policies and guidance for the management of the historic environment', 2008. Available at: <https://content.historicengland.org>.

- uk/images-books/publications/conservation-principles-sustainable-management-historic-environment/conservationprinciplespoliciesguidanceapr08web.pdf
2. D Thickett, F David and N Luxford, 'Air exchange rate: a dominant parameter for showcases', *The Conservator*, pp 19-34, 2006.
  3. ASTM E 976-84, 'Standard guide for determining the reproducibility of acoustic emission sensor response', 1988.
  4. G Accardo, C Caneva and S Massa, 'Stress monitoring by temperature mapping and acoustic emission analysis: a case study of Marcus Aurelius', *Studies in Conservation*, Vol 28, pp 67-74, 1983.
  5. M Strojceki, M Łukomski, L Krzemień, J Sobczyk and Ł Bratasz, 'Acoustic emission monitoring of an eighteenth-century wardrobe to support a strategy for indoor climate management', *Studies in Conservation*, Vol 59, pp 225-239, 2014.
  6. S A MacDonald, C R Schardt, D J Maisiello and J H Simmons, 'Dispersion analysis of FTIR reflection measurements in silicate glasses', *Journal of Non-Crystalline Solids*, Vol 275, pp 72-82, 2000.
  7. L Robinet, K Eremin, S Fearn, C Pulham and C Hall, 'Understanding glass deterioration in museum collections through Raman spectroscopy and SIMS analysis', *Material Research Society Symposium*, P852, pp 121-128, 2005.
  8. D Thickett, 'Epidemiology: the missing link', Submitted to 18th Triennial Conference of ICOM-CC.
  9. R H Brill, 'Chemical analyses of early glasses', *The Corning Museum of Glass*, New York, 1999.
  10. C S Cheung, M Spring and H Liang, 'Ultra-high-resolution Fourier domain optical coherence tomography for old master paintings', *Optics Express*, Vol 23, No 8, pp 10145-10157, 2015. <https://doi.org/10.1364/OE.23.010145>
  11. C S Cheung, J M O Daniels, M Tokurakawa, W A Clarkson and H Liang, 'High-resolution Fourier domain optical coherence tomography in the 2  $\mu\text{m}$  wavelength range using a broadband supercontinuum source', *Optics Express*, Vol 23, No 3, pp 1992-2001, 2015. <https://doi.org/10.1364/OE.23.001992>